Int. J. Solids Structures Vol. 30, No. 8, pp. 1075–1092, 1993
Printed in Great Britain

0020–7683/93 $6.00 + .00
Pergamon Press Ltd

CREEP BUCKLING OF VISCOELASTIC STRUCTURES

T. M. MINAHEN†
Department of Aeronautics, California Institute of Technology, Pasadena, CA 91125, U.S.A.

and

W. G. KNAUSS
Department of Aeronautics and Applied Mechanics, California Institute of Technology, Pasadena, CA 91125, U.S.A.

(*Received* 5 *May* 1992; *in revised form* 4 *October* 1992)

Abstract—The creep buckling of viscoelastic structures is investigated analytically and experimentally. The theory of linear viscoelasticity is used to model polymeric column specimens subjected to constant compressive end loads. The growth of initial imperfections is calculated using the hereditary integral formulation. Solution techniques are developed for small displacements and also generalized to include the effects of non-linear kinematics. It turns out that the kinematically linear model represents the deformation process closely and conservatively; material non-linearities are not dominant since maximum strains of the order of only 2% are encountered. The analyses are exact with respect to (non-linear) kinematics and linearly viscoelastic material representation. A failure criterion based on maximum deformation allows the column life to be determined from the material relaxation modulus if the initial imperfections are known. A discussion on the possible generalization of the results to include plates and shells is presented.

Results of creep buckling experiments performed on PMMA specimens at elevated temperatures (accelerating the creep behavior) are reported. The relaxation modulus of PMMA is represented by a Prony–Dirichlet series and the model is used to simulate the laboratory experiments. Model and experimental results are compared and discussed especially with respect to uncontrollable material behavior.

1. INTRODUCTION

Providing for structural stability in engineering designs is a concern of long standing. With trends in aerospace applications of composite materials oriented towards high temperature use a question arises with regard to their performance over prolonged periods of time. Especially with the possible application of thermoplastics-based composites the long-term development of structural instability under a variety of circumstances (prolonged high temperature exposure) adds to time dependent failure modes in composite structures. In this paper we examine the problem of buckling of a linearly viscoelastic column as an illustration of the evolution of the transverse instability in more complicated structures such as plates and shells.

The advent of polymer based composites and their mechanical response sensitivity at elevated temperatures introduces the viscoelastic response into possible long-term structural behavior. It is particularly important to examine the methods of predicting long-term behavior (months, years) on the basis of either fundamental material properties or by deduction from relatively short-term tests. Failures of interest here are those that lead to global instability in the classical structural sense (struts, plates, shells) as well as local instabilities associated with composite delamination. The latter may result from local damage and inhomogeneous stresses associated with bending and thermal gradients through a structural member. Moreover, the problem of fiber crimping as a time-dependent problem of elastic fibers buckling in a viscoelastic matrix is of interest inasmuch as the intrinsic time dependence of the instability problem derives from the polymer properties and one would expect to understand the evolution of that kind of damage once the more basic problem is more fully delineated.

The first attempt at addressing creep buckling was probably offered by Freudenthal

† Current address: School of Mechanical and Aerospace Engineering, Oklahoma State University, Stillwater, OK 74078, U.S.A.

(1946) who considered the buckling of a column possessing the properties of a Maxwell material. While he formulated the problem in terms of a power series expansion, postulating the series divergence as indicating loss of stability, it was pointed out by Kempner and Pohle (1953) that the coefficients of the series were incorrect and that a critical time as posed by Freudenthal did not exist. Hilton (1952) used the Shanley criterion of loss of moment equilibrium (collapse) for a Maxwell material model and for a standard linear solid. Geophysical interests, including those of Biot (1959, 1961) and Sherwin and Chapple (1968) centered on the folding of mineral veins and tectonic layers; these developments up to 1962 are well summarized in Kempner's review (1962). Flügge addressed the same problem with more advanced material models by attacking the problem in the Laplace domain (1975) without, however, developing the fully time-dependent response. Prospects of space re-entry heating led Libove (1952), and Hoff (1954, 1956) to study the buckling of high temperature aluminum alloys. Huang (1976) revisited the Libove and Hoff problems under inclusion of large deformations and power law hardening plasticity as well as second phase creep. The most recent analysis by Bodner (1991) addresses the effect of creep in the presence of (metal) yielding to explore apparent paradoxes of buckling in the plastic range. Also, Schapery (1987) has addressed the linearly viscoelastic buckling problem in relation to ice folding, primarily in the Laplace domain and showed that the long term growth of the deflection has exponential character. To determine the complete history he suggests the (numerically possibly unstable) inversion of the Laplace transform or taking recourse to earlier established approximate analysis methods.

Our aim in this work is directed at formulating the problem exactly within the realm of linear viscoelasticity and at the same level of kinematics as the classical Euler buckling problem. Under these precepts the resulting solution would be "exact" and experimental verification would seem unnecessary. In fact, the analysis is available to explore the sensitivity of the process of instability evolution subject to variation in any of the problem parameters. However, in the interest of examining the degree of agreement between analysis and controlled conditions in a laboratory environment we report also on experimental corroboration.

Buckling of elastic structures is most often discussed in the context of a bifurcation or eigenvalue problem. The question has been considered whether for the time dependent problem a similar formulation exists such that a perfectly straight, slender column experiences lateral deformation under axial load after some (critical) time, which deformation then grows at a determinable rate. We have not approached the problem in this manner, but rather, after discussion with various colleagues follow the understanding, expressed by Tvergaard (1985) with respect to rate sensitivity of elasto-plastic materials, that the instability problem takes the form of time dependent response of an initially imperfect structure. In this spirit we formulate the deformation problem in the next section, followed in Section 3 with the complete, closed form solution for a standard linear solid as a benchmark, since the general solution, delineated in Section 4, needs to draw on numerical methods. Section 5 deals with the effect of large deformations for the same problem to illustrate that this complication does not, in effect, invalidate the conclusions, drawn in the subsequent section, on the basis of the linearized analysis. Section 6 relates the results to observations on quasi-elastic arguments and bounds the time to achieve critical deformations, it also points to generalized deductions applicable to structures of widely different shapes. Finally, we conclude this presentation with an experimental examination and comparison of the analytical results with experimental observations.

2. FORMULATION OF THE PROBLEM

Consider a simply-supported beam/column of unit depth subjected to compressive loads applied at the end points of its neutral axis and lateral loads applied normal to the beam axis. The column neutral axis possesses an initial profile $w_0(x)$ as indicated in Fig. 1 along with the full coordinate definitions and appropriate displacement components. Axial strains are associated with the axial displacement $u_0(x, t)$ which will be presumed to remain small compared to the column length. Denoting the additional deflection by $w(x, t)$ and

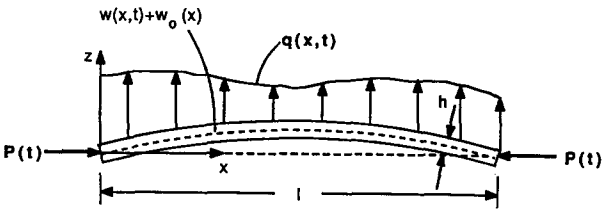

Fig. 1. Problem geometry.

allowing, for the present, only small section rotations, one finds the strain ε_{xx} from

$$\varepsilon_{xx}(x,z,t) \equiv \varepsilon(x,z,t) = \frac{\partial u(x,z,t)}{\partial x} = \frac{\partial u_0(x,t)}{\partial x} - z\frac{\partial^2 w(x,t)}{\partial x^2}. \tag{1}$$

Using the convolution form of the unidirectional constitutive behavior and disregarding inertia effects, one derives from the equilibrium of bending moments the relation

$$-\frac{h^3}{12}\int_{-\infty}^{t} E(t-\xi)\frac{\partial^5 w(x,\xi)}{\partial^4 x\,\partial\xi}\mathrm{d}\xi = P(t)\left[\frac{\partial^2 w(x,t)}{\partial x^2} + \frac{\mathrm{d}^2 w_0(x)}{\mathrm{d}x^2}\right] \tag{2}$$

subject to the boundary conditions

$$w(0,t) = w(l,t) = 0, \quad M(0,t) = M(l,t) = 0. \tag{3a, b}$$

Different boundary conditions than these can be accommodated equally well so that the current development is applicable to other column buckling problems and, in fact, the results developed here are readily generalized for these different problems (see Section 6). The boundary value problem in eqns (2) and (3a, b) is solved in terms of a Fourier series by letting

$$w(x,t) = \sum_{m=1}^{\infty} A_m(t)\sin\frac{m\pi x}{l}, \quad w_0(x) = \sum_{m=1}^{\infty} B_m \sin\frac{m\pi x}{l}. \tag{4a, b}$$

Use of these expansions in (2) renders an equation which satisfies it term-by-term, and upon non-dimensionalizations in the forms

$$P_e(t) \equiv \frac{E(t)h^3\pi^2}{12l^2}, \tag{5a}$$

$$p(t) \equiv \frac{P(t)}{P_e(0)}, \quad r(t) \equiv \frac{E(t)}{E(0)}, \tag{5b, c}$$

$$\alpha_m(t) \equiv \frac{A_m(t)}{h}, \quad \beta_m \equiv \frac{B_m}{h}, \tag{5d, e}$$

the governing integral equation becomes

$$-m^2 r(t)\alpha_m(0^+) - m^2\int_{0^+}^{t} r(t-\xi)\frac{\mathrm{d}\alpha_m(\xi)}{\mathrm{d}\xi}\mathrm{d}\xi + p(t)\alpha_m(t) + p(t)\beta_m = 0, \tag{6}$$

the solution of which allows the construction of the lateral displacement $w(x, t)$ on a mode-by-mode basis. The solution of this Volterra integral equation presents, in general, no mathematical problem, though the means of solution depends strongly on the mathematical

representation of the relaxation function $E(t)$. While the stability problem for general and realistic material behavior demands ultimately numerical methods (see Section 4) we turn first briefly to the solution for the simple material representation of a standard linear solid, for which a solution may be obtained in closed form. The generalization of this latter approach to increasingly more complex material representations is, analytically speaking possible, but the analytical/numerical involvement is, in our estimation, as large or larger than the numerical effort delineated in Section 4.

Kempner (1954) has dealt with the standard linear solid in buckling. We delineate the subsequent analysis here because the closed-form solution in terms of the convolution integral allows us to gage the accuracy and reliability of the numerical process used in Section 4, since the numerical interpretation of functions involving relaxation or creep behavior extending over many decades of time has demanded, in our past experience, special precision and/or convergence considerations.

3. EXAMPLE FOR THE STANDARD LINEAR SOLID

The standard linear solid has the important short and long time characteristics experienced in the behavior of many engineering polymers. The mechanical analog of this material model is a linearly elastic element in parallel with a Maxwell material model. In the typical vernacular of viscoelastic material description we refer to the "glassy buckling load" as the Euler load computed with the short term (glassy) modulus $E(0)$, while the term "rubbery buckling load" refers to the Euler load based on the long term modulus $E(\infty)$.

We begin by differentiating the equilibrium equation (6) with respect to time, rendering

$$-m^2\dot{r}(t)\alpha_m(0^+)-m^2\int_{0^+}^{t}\dot{r}(t-\xi)\frac{\mathrm{d}\alpha_m(\xi)}{\mathrm{d}\xi}\,\mathrm{d}\xi-m^2r(0)\dot{\alpha}_m(t)$$
$$+\dot{p}(t)\alpha_m(t)+p(t)\dot{\alpha}_m(t)+\dot{p}(t)\beta_m=0 \quad (7)$$

where the dot [e.g. $\dot{r}(t-\xi)$] implies differentiation with respect to the argument. The isothermal relaxation modulus of a standard linear solid in its normalized form is

$$r(t)=r_\infty+r_1\,\mathrm{e}^{-\lambda t},\quad r(0)=r_1+r_\infty=1. \quad (8)$$

Since, by virtue of (8)

$$\dot{r}(t-\xi)=-\lambda r(t-\xi)+\lambda r_\infty, \quad (9)$$

combining (6), (7) and (9) yields a linear differential equation for the growth of each buckling mode as

$$[p(t)-m^2]\dot{\alpha}_m(t)+[\dot{p}(t)+\lambda p(t)-\lambda m^2r_\infty]\alpha_m(t)+\dot{p}(t)\beta_m+\lambda p(t)\beta=0, \quad (10)$$

where $r(0)=1$ has been used. This equation may be solved analytically for simple forms of the loading function, $p(t)$. For constant end loading, $p(t)=p_0$, eqn (10) becomes

$$[p_0-m^2]\dot{\alpha}_m(t)+\lambda[p_0-m^2r_\infty]\alpha_m(t)+\lambda p_0\beta_m=0, \quad (11)$$

which has the solution for $p_0<1$

$$\alpha_m(t)=\left[\alpha_m(0^+)+\frac{p_0\beta_m}{p_0-m^2r_\infty}\right]\exp\lambda\left(\frac{p_0-m^2r_\infty}{m^2-p_0}\right)t-\frac{p_0\beta_m}{p_0-m^2r_\infty}. \quad (12)$$

The nature of this solution depends on the magnitude of p_0; there are three distinct cases:

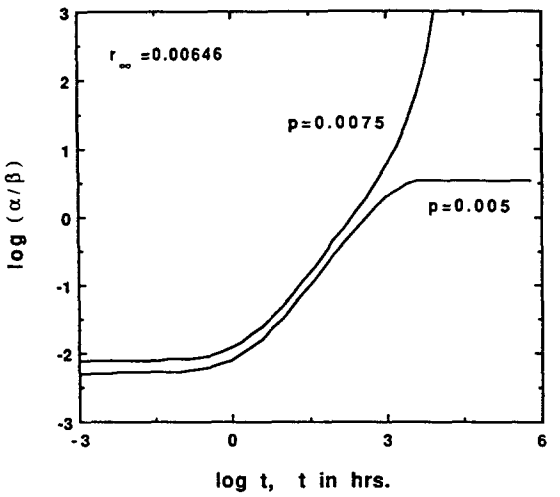

Fig. 2. Constant end load response of standard linear solid column.

(1) when $p_0 < m^2 r_\infty$, i.e. when the load is less than the "rubbery buckling load" for the mth deformation mode, the response exhibits a decaying exponential term and asymptotically approaches a long term equilibrium state;

(2) when $m^2 r_\infty \leqslant p_0 < m^2$ the response has a growing term† and creep instability occurs;

(3) when $m^2 \leqslant p_0$ immediate or "glassy buckling" occurs.

Solutions of eqn (12) for the lowest mode ($m = 1$) and for two different end loads are plotted in Fig. 2, where an evaluation of (12) was made assuming‡ $r_\infty = 0.00646$ and $\lambda = 0.23$ hr s^{-1}. For $p_0 = 0.0005$ equilibrium is approached asymptotically since $p_0 < r_\infty$. For $p_0 = 0.0075$, however, creep buckling occurs, leading to unbounded deflections as time progresses. Shown in the figure are the responses of the mode $m = 1$ to the indicated loading.

Of significant practical importance are the growth rates of the deformation modes, for these rates determine which of the modes will ultimately dominate the deformation process. We consider the case $r_\infty < p_0/m^2 < 1$. Defining g as the growth exponent

$$g(m, p_0) = \lambda \frac{p_0 - m^2 r_\infty}{m^2 - p_0}, \tag{13}$$

we see that it is a discrete, decreasing function of the mode number m, but increasing in the load p_0 and becomes unbounded as $p_0/m^2 \to 1.0$.

It is seen that the lowest deformation mode grows the fastest and that as the glassy buckling load for the first mode is approached from below its growth rate becomes unbounded. Thus, as the glassy buckling load of the first mode is approached the first mode grows infinitely faster than the higher modes. However, even when p_0 approaches the rubbery buckling load from above, the growth rate of the first mode is still significantly higher than those of the higher modes. For example, if one considers only load cases in which at least two modes grow unboundedly, it can be shown that for $r_\infty < 0.25$ the ratio of growth exponents, $g(1, p_0)/g(2, p_0)$ has a minimum with respect to load. This minimum approaches 4.0 as $r_\infty \to 0$ and becomes unbounded as $r_\infty \to 0.25$§. From this assessment it is seen that for significant deformations (unless the $m = 1$ component of the geometric

† The growth is exponential for $p_0 > m^2 r_\infty$ and proportional to t when $p_0 = m^2 r_\infty$.

‡ This value is characteristic of the long term plateau behavior for medium molecular weight polymethylmethacrylate.

§ $r_\infty = 0.25$ corresponds to the case when "glassy buckling load" for the first mode equals "rubbery buckling load" for the second mode.

imperfection is identically zero) the time response of the first mode will dominate the column response.

Having summarized analytically and in closed form the most important features of the buckling/deformation behavior for a simple viscoelastic solid, we use these results to guarantee that the numerical integration scheme derived in the next section renders reliable results.

4. THE CASE OF REALISTIC MATERIAL PROPERTIES

There are two readily available methods for the numerical integration of eqn (6): The discretization of the integral (Hopkins and Hamming, 1957), renders a matrix equation of (nearly) triangular form which is readily solvable. For details on its formulation for this problem the reader is referred to Minahen (1992).

4.1. *The numerical scheme*

The method adopted subsequently (Taylor *et al.*, 1970), draws on the (customary) representation of the relaxation modulus in terms of a Prony–Dirichlet series

$$r(t) = r_\infty + \sum_{i=1}^{n} r_i \mathrm{e}^{-\lambda_i t}; \quad r(0) = 1, \tag{14}$$

where r_∞ and $r(0) \equiv r_g$ represent again the long term (rubbery) and short term (glassy) moduli. With the subdivision of the range of integration into discrete intervals t_j in mind, consider the integral $I(t_j)$ along with its approximation which substitutes the average of $\alpha_m(t)$ over the interval in place of its continuously varying value;

$$I_j \equiv I(t_j) = \int_{0^+}^{t_j} r(t_j - \xi) \frac{\mathrm{d}\alpha_m(\xi)}{\mathrm{d}\xi} \mathrm{d}\xi \simeq \sum_{k=1}^{j} r(t_j - t_{k-1}) \left.\frac{\mathrm{d}\alpha_m(\xi)}{\mathrm{d}\xi}\right|_{\xi = t_k} \Delta t_k, \tag{15}$$

for sufficiently small intervals this approximation is of little consequence. Using a difference approximation for the time derivative

$$\left.\frac{\mathrm{d}\alpha_m(\xi)}{\mathrm{d}\xi}\right|_{\xi = t_k} \simeq \frac{\Delta\alpha_m^k}{\Delta t_k}, \tag{16}$$

and upon using eqns (14) and (16) in (15) one finds

$$I_j \simeq \left[r_\infty + \sum_{i=1}^{n} r_i \mathrm{e}^{-\lambda_i (t_j - t_{j-1})} \right] \Delta\alpha_m^j + r_\infty (\alpha_m^{j-1} - \alpha_g) + \sum_{i=1}^{n} r_i \mu_{ij}, \tag{17}$$

where we have used

$$\mu_{ij} = \sum_{k=1}^{j-1} \mathrm{e}^{-\lambda_i (t_j - t_{k-1})} \Delta\alpha_m^k \quad \text{and} \quad \alpha_m^{j-1} \simeq \sum_{k=1}^{j-1} \Delta\alpha_m^k + \alpha_g. \tag{18}$$

μ_{ij} can also be written for recursive use as

$$\mu_{ij} = \mathrm{e}^{-\lambda_i (t_j - t_{j-2})} \Delta\alpha_m^{j-1} + \mathrm{e}^{-\lambda_i (t_j - t_{j-1})} \mu_{ij-1}. \tag{19}$$

The evolution equation (6) can now be written at time $t = t_j$ with the help of (17)–(19) as

$$-m^2 r(t_j)\alpha_m(0^+) - m^2 I_j + p(t_j)\alpha_m^j + p(t_j)\beta_m = 0, \tag{20}$$

which, with

$$\alpha_m^j = \alpha_m^{j-1} + \Delta\alpha_m^j \tag{21}$$

Table 1. Prony–Dirichlet series parameters for PMMA at 75°C

Relaxation Modulus Parameters			
$\log E_i$ dynes cm^{-2}	$\log (1/\lambda_i)$ seconds	$\log E_i$ dynes cm^{-2}	$\log (1/\lambda_i)$ seconds
9.2333	−5.556	9.7067	2.444
9.5386	−3.556	9.4562	3.444
9.2238	−2.556	9.0211	4.444
9.5556	−1.556	7.9474	5.444
9.3217	−0.556	7.3965	6.444
9.5394	0.444	6.9026	7.444
9.4271	1.444	$\log E(\infty)$	8.260

renders

$$p(t_j)[\Delta\alpha_m^j+\alpha_m^{j-1}]-m^2\left[r_\infty+\sum_{i=1}^{n} r_i\,e^{-\lambda_i(t_j-t_{j-1})}\right]\Delta\alpha_m^j = m^2 r_\infty(\alpha_m^{j-1}-\alpha_g) - p(t_j)\beta_m+m^2 r(t_j)\alpha_m(0^+)+m^2\sum_{k=1}^{n} r_i\mu_{ij}, \quad (22)$$

for the increment of the non-dimensional amplitude of the mth deformation mode, which may be extracted explicitly as

$$\Delta\alpha_m^j = \frac{1}{p(t_j)-m^2 r_\infty - m^2\sum_{i=1}^{n} r_i\,e^{-\lambda_i(t_j-t_{j-1})}} \times\left\{m^2 r(t_j)\alpha_m(0^+)+m^2 r_\infty(\alpha_m^{j-1}-\alpha_g)+m^2\sum_{i=1}^{n} r_i\mu_{ij}-p(t_j)[\alpha_m^{j-1}+\beta_m]\right\}, \quad (23)$$

with the total amplitude of the mth mode α_m^j at time t_j being computed from eqn (21).

4.2. *Application to a column of PMMA*

We choose PMMA (polymethylmethacrylate) as a model material because it possesses viscoelastic properties typical of thermoplastic polymers and because, with suitable temperature control, experiments can be performed in the laboratory on a reasonable time scale.† The exponential series representation for the relaxation modulus is given in Table 1 and compared with the experimental data (centers of the symbols) in Fig. 3.

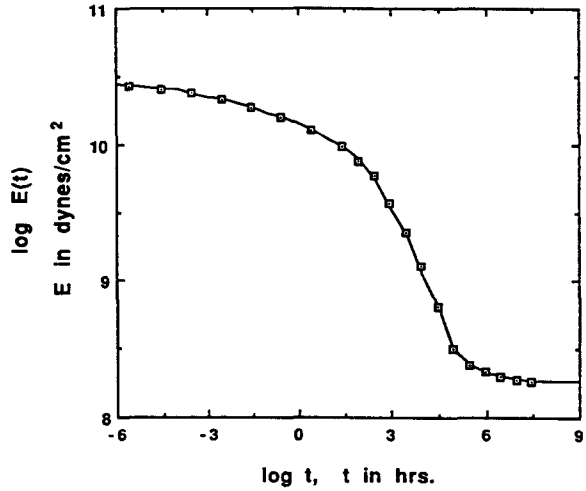

Fig. 3. PMMA relaxation modulus at 75°C.

† Although in its commercial and uncrosslinked form PMMA does not possess a true long term or "rubbery" modulus, we consider its rubbery plateau to represent this property; the issue does not arise in the experimental work.

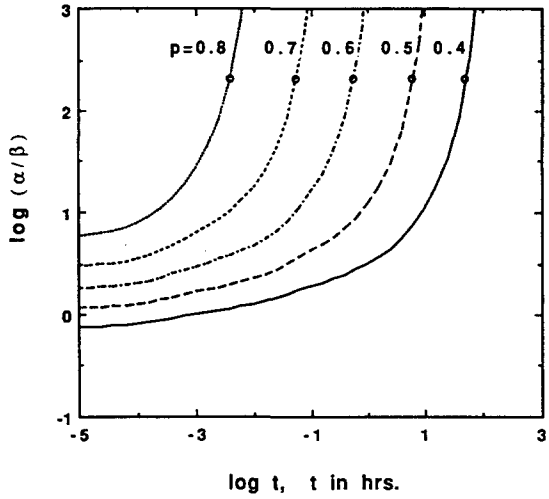

Fig. 4. Load sensitivity for PMMA column.

For the numerical evaluation we limit ourselves to computing the evolution of only the first mode ($m = 1$) because, as shown for the standard linear solid, the higher modes develop at a slower rate as long as β_1 is not identically equal to zero. Before examining the results of the computations we note that the solution to eqn (6) is a linear function of the initial imperfection (β_m); we shall recall this result in connection with the experimental work.

Figure 4 shows the development of the (fundamental mode) amplitude for five different load levels to illustrate the continuous imperfection growth. As pointed out by Kempner (1954) and in Section 3 for the simple solid, and by Schapery (1987) for more complex materials, there is no natural time (limit) at which "dynamic" conditions take over, and the criterion as to when failure is accomplished must be based on either load carrying ability (3), or on a criterion of maximally achieved deflection. In the present example of time-constant loading, loss of load carrying ability is not predicted by the linearized theory, nor is it by the fully non-linear theory, for the same reason as shown later. We define "failure" of the column, therefore, as the achievement of a critical displacement, say, a certain percentage of the beam thickness h or of its length L. For the present discussion we choose a critical deflection as $2.4h$. This value is marked in Fig. 4 by small circles; upon cross-plotting the corresponding times t_c achieved for different values of applied load one obtains the result shown in Fig. 5 as curve "A." It can be seen that large changes in time dependent

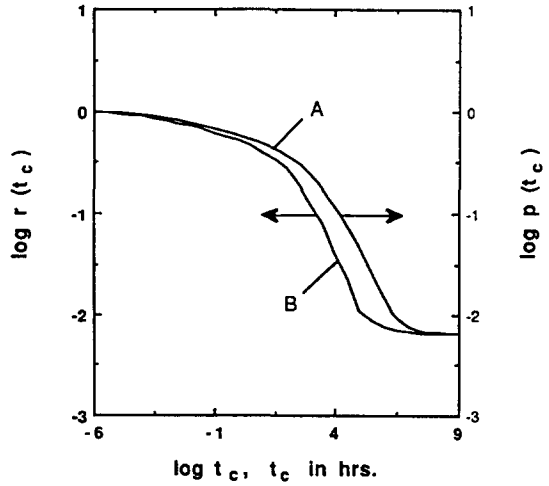

Fig. 5. "Buckling times" for PMMA columns.

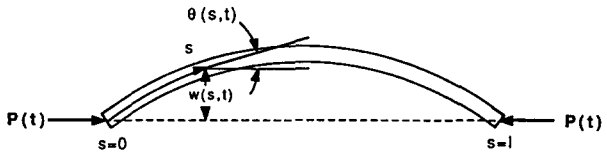

Fig. 6. Geometry for the visco-elastica.

behavior can result from relatively small changes in the load level. If the times t_c are accepted as the "buckling times" then Fig. 5 represents the time dependence of the column failure under axial loading.

So far we have examined the column deformation behavior under the restriction of small deformations, specifically small section rotations. This assumption leads naturally to unbounded deflections of the column which result is not only physically unappealing but raises the question whether large deformation alters the time response significantly.

5. THE VISCO-ELASTICA PROBLEM

For the large deformation formulation we retain the linearly viscoelastic behavior and assume for this development that strains remain sufficiently small to admit that material description. This assumption will have to be verified after the analysis is complete.

Let $\theta(s, t)$ represent the section rotation at position s along the column, (*cf.* Fig. 6) the latter being measured as the arclength. In place of eqn (1) one now has

$$\varepsilon(s, z, t) = \varepsilon_0(s, t) - z\frac{\partial\theta(s, t)}{\partial s}, \tag{24}$$

so that the counterpart of eqn (6) becomes, in non-dimensional form†

$$-r(t)\frac{\partial^2\theta(\zeta, t)}{\partial s^2}\bigg|_{t=0^+} - \int_{0^+}^{t} r(t-\xi)\frac{\partial^3\theta(\zeta, \xi)}{\partial\zeta^2\,\partial\xi}\,\mathrm{d}\xi = p(t)\pi^2[\sin\theta(\zeta, t) + \sin\theta_0(\zeta)] \tag{25}$$

and the boundary conditions of vanishing end moments (simple supports) as

$$\frac{\partial\theta(s, t)}{\partial s}\bigg|_{s=0} = \frac{\partial\theta(s, t)}{\partial s}\bigg|_{s=l} = 0 \tag{26}$$

and

$$w(0, t) = \omega(l, t) = 0. \tag{27}$$

The lateral deflection at $s = l/2$ is written as

$$w(l/2, t) = \int_0^{l/2} \sin\theta(s, t)\,\mathrm{d}s. \tag{28}$$

The visco-elastica problem is a two-point boundary value problem, which will also be solved numerically for realistic material properties of PMMA.

We summarize here briefly the development for the material representation by a Prony series, referring the reader for more detail to Minahen (1992). The integral in eqn (25) is approximated by

$$J_j(\zeta) \equiv J(\zeta, t_j) \simeq \sum_{k=1}^{j} r(t_j - t_{k-1})\frac{\partial^3\theta(\zeta, \xi)}{\partial\zeta^2\,\partial\xi}\bigg|_{\xi=t_k}\Delta t_k. \tag{29}$$

† arclength has been normalized using column length.

Applying a differencing scheme to approximate the time derivative and denoting spatial derivatives by a superscripted prime [e.g. $\theta'(\zeta, t)$] gives

$$J_j(\zeta) \simeq \left[r_\infty + \sum_{i=1}^{n} r_i \mathrm{e}^{-\lambda_i(t_j - t_{j-1})} \right] \Delta\theta_j''(\zeta) + r_\infty [\theta_{j-1}''(\zeta) - \theta_g''(\zeta)] + \sum_{i=1}^{n} r_i v_{ij}(\zeta), \tag{30}$$

where the Prony series representation [eqn (14)], of the relaxation modulus has been used as well as the definition

$$v_{ij}(\zeta) \equiv \sum_{k=1}^{j-1} \mathrm{e}^{-\lambda_i(t_j - t_{k-1})} \Delta\theta_k''(\zeta). \tag{31}$$

By using techniques similar to those used in the analysis of the geometrically linear model, v_{ij} can be put into a recursive form

$$v_{ij}(\zeta) = \mathrm{e}^{-\lambda_i(t_j - t_{j-2})} \Delta\theta_{j-1}''(\zeta) + \mathrm{e}^{-\lambda_i(t_j - t_{j-1})} v_{ij-1}(\zeta). \tag{32}$$

Upon substitution of eqns (30) and (31) into eqn (25) a non-linear ordinary differential equation in ζ results in

$$\Delta\theta_j''(\zeta) \simeq \frac{-1}{r_\infty + \sum_{i=1}^{n} r_i \mathrm{e}^{-\lambda_i(t_j - t_{j-1})}} \left\{ r_\infty [\Delta\theta_{j-1}''(\zeta) - \theta_g''(\zeta)] + \sum_{i=1}^{n} r_i v_{ij}(\zeta) \right.$$
$$\left. + p(t_j)\pi^2 [\sin\theta_{j-1}(\zeta) + \Delta\theta_j(\zeta)] + \sin\theta_0(\zeta) \right\}, \tag{33}$$

which is solved numerically using the shooting method to iterate on a solution at each time step. A fourth order Runge–Kutta integration scheme with adaptive step size is used to integrate from $s = 0$ to $s = l$. The result of the numerical evaluation of eqn (33) renders the results shown in Fig. 7. Suppose that for present purposes one defines failure again as the achievement of the maximum deflection; from a practical point of view the attainment of this condition is way past practical significance for "buckling descriptions" because it implies that the column arc shortening is such that the two ends touch. Two observations are then in order. As expected the solution follows the linearized behavior for a substantial fraction of the deformation history. Second, it is clear that the linearized version provides

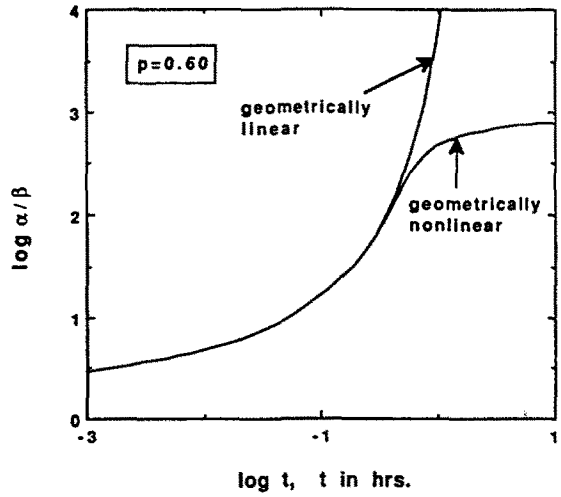

Fig. 7. Response of PMMA visco-elastica.

failure times which are on the conservative side of any real estimate. This observation would seem important in interpreting the buckling behavior of viscoelastic structures.

6. EVALUATION OF RESULTS AND GENERALIZATIONS

We return to the results of the linearized solution, in particular to Fig. 5 and note that the plot of applied load against the time to failure (t_c) looks like the relaxation modulus normalized by its glassy value; this function is also shown in Fig. 5 as curve "B". For the realistic material these two curves turn out to be identical except shifted relative to each other along the logarithmic time axis.† Thus the failure time for time invariant axial loading may be approximated by a formula simulating the quasi-elastic buckling behavior of simply-supported columns in the form

$$\delta_c \equiv \alpha(t_c) \simeq \frac{p_0(t_c)\beta}{r(\phi t_c) - p_0(t_c)}, \tag{34}$$

where δ_c is the critical deflection. We have remarked earlier that for loads obeying the inequality $p_0 < r_\infty$, a stable deformation results. While this latter condition implies that displacements will not grow without bound below this level, it does leave open the question whether a critical displacement will, nevertheless, be achieved in a finite time. Clearly, there will be some load level below r_∞ which may satisfy the critical displacement criterion, and that load will depend on the magnitude of the critical displacement chosen. We do not pursue this issue further in detail, but refer to this inequality as providing the (approximately) lower instability boundary.

Returning to eqn (34) we note that the shift factor ϕ multiplying the failure time t_c depends on the size of the critical displacement chosen; because of the proportionality of the deformations to the initial imperfection, the dependence of the shift ϕ depends also, in a simple way on this quantity. If it could be shown that its value is generally smaller than unity one would deduce that a choice of unity of this factor (no shift) would always lead to conservative time estimates through the quasi-elastic formula

$$\delta_c \equiv \alpha(t_c) = \frac{p_0(t_c)\beta}{r(t_c) - p_0(t_c)}, \tag{35}$$

which is the simple Euler formula with Young's modulus replaced by the relaxation modulus as a function of the failure time t_c. An answer to this question could be provided by repeated computations as those shown in Fig. 5 with various ratios of critical deflections to the initial imperfection. Instead of offering this numerical development we choose to elucidate a simple though explicit result in terms of the standard linear solid. Recalling eqn (12) and writing it for $\alpha(t_c) = \delta_c$ yields

$$\delta_c = \alpha(t_c) = \left[\frac{p_0\beta}{1-p_0} + \frac{p_0\beta}{p_0 - r_\infty}\right] \exp \lambda\left(\frac{p_0 - r_\infty}{1-p_0}\right) t_c - \frac{p_0\beta}{p_0 - r_\infty}. \tag{36}$$

It follows that

$$t_c = \frac{1}{\lambda}\frac{1-p_0}{p_0 - r_\infty} \ln \left[\frac{1 + \frac{\delta_c}{\beta}\left(1 - \frac{r_\infty}{p_0}\right)}{1 + \frac{p_0 - r_\infty}{1-p_0}}\right]. \tag{37}$$

† The relaxation modulus appears "bumpy" as a result of the Prony–Dirichlet series representation.

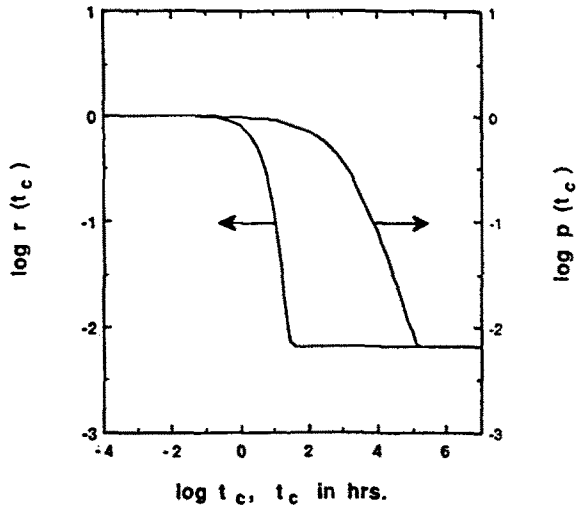

Fig. 8. Buckling time for standard liner solid.

A plot of the buckling time as a function of applied load is shown in Fig. 8. The material properties used in the curve are the same as used in Section 3 and the normalized relaxation modulus of the material is also plotted in Fig. 8.

Two observations are evident from the figure: first if one were to estimate the buckling time using the normalized relaxation modulus in place of the actual buckling time curve the error would be conservative by about three orders of magnitude, and, second, for the simple material model the predicted buckling time curve is not represented by the relaxation curve shifted along the log-time axis as was the case for the results based on the properties for a real material, PMMA. This observation is in keeping with results from other viscoelasticity problems (Schapery, 1962), and hinges on the rate with which viscoelastic properties change with $\log_{10} t$ in the transition region. We next use eqn (37) to demonstrate explicitly how the shifting between the relaxation function and the curve representing the buckling failure depends on the critical displacement and the initial imperfection. We do this by estimating the time scales for the two curves when either $r(t)$ or $p(t_c)$ have dropped by 1/e of the initial value (*cf.* Fig. 8). From eqn (8) one has then [$r(0) = 1$]

$$r_\infty + r_1 \mathrm{e}^{-\lambda(t_c)_r} = \frac{1}{e}; \quad r_1 = 1 - r_\infty, \tag{38}$$

which, because $r_\infty \ll 1/3$, $r_1 \simeq 1$ yields

$$(t_c)_r = \frac{1}{\lambda}, \tag{39}$$

while the failure time determined from eqn (37) with $p_0 = 1/\mathrm{e}$ yields

$$(t_c)_p = \frac{1}{\lambda}(\mathrm{e}-1)\ln\left[\frac{\mathrm{e}-1}{\mathrm{e}}\left(1+\frac{\delta_c}{\beta}\right)\right] \tag{40}$$

or, if $\mathrm{e} \simeq 3$,

$$(t_c)_p \simeq \frac{1}{\lambda}\ln\left[\frac{2}{3}\left(1+\frac{\delta_c}{\beta}\right)\right]^2. \tag{41}$$

The shift factor ϕ between the curves for buckling failure and relaxation response is thus

$$\phi \simeq \ln\left[\frac{2}{3}\left(1+\frac{\delta_c}{\beta}\right)\right]^2, \tag{42}$$

which, since typically $\delta_c/\beta \gg 1$ renders a logarithmic dependence on the ratio δ_c/β. It is interesting to note that the shifting depends on the non-dimensional ratio of the final or maximal (δ_c) to initial or minimal (β) column deflection.

At this point it is of interest to observe that in 1969, Halpin and Meinecke (1969) examined experimentally the proposition that the buckling load of a viscoelastic column be given by the quasi-elastic result embodied in eqn (35). While several of the tests conducted under different load levels and at different temperatures seemed to follow that behavior to some extent, a portion of the tests did not conform to that relation. In light of the present results it seems that the initial imperfection needs to be considered in the determination of the "buckling time" and since that fact was not consistently accounted for in these early experiments (initial deformations were assumed to vanish), one should not expect a unique relation between the applied load and the "time", however consistent the latter may have been defined.

Finally we note that the sensitivity of the "buckling time" to the initial imperfections is not very strong. To clarify this statement we refer to Fig. 4 and note that an increase in the initial imperfection by a factor of 10 moves any of the curves downward along the ordinate by a unit. Because of the (increasing) steepness of these curves in the vicinity of the deflection designated as critical deflection such a vertical shift does not produce much of a change along the log-time axis; in fact, that change in time amounts only to a factor on the order of about 1.5 for this example. Hoff (1956) has made similar observations on creep buckling though he dealt with the nonlinear creep appropriate for metallic structures for which he found that a tenfold change in the imperfection size resulted in a change in the time-to-failure given by a factor on time on the order of only 2.

6.1. *Generalization to other structures*

It is useful to consider the implication of the results in this section to columns with other boundary conditions and to plate and shell configurations. While detailed results have to be reserved for further and more detailed investigations, the following general observations are in order, on the basis of analogy to the buckling of the elastic counterparts.

With respect to columns subject to different boundary conditions it is clear that identical results prevail as long as integer multiples or subdivisions of the column length produces boundary conditions contained in the present solution. The cases of other end supports can be treated in a similar manner. Guided by the simply-supported solution where the first mode rapidly dominates the deformation response one can readily perform the creep buckling response analyses for other boundary conditions. In this case the normalized quasi-static equilibrium equation is identical to that of the simply-supported column [eqn (6) written for $m = 1$] when the end load is normalized by the glassy buckling load. For the case of elastic plates and shells the equilibrium equations depend on the elastic modulus as well as the bending modulus of rigidity

$$D = \frac{Eh^3}{1-\nu^2}. \tag{43}$$

If one allows for constant Poisson's ratio,† a not unreasonable approximation if one is interested in nearly rigid behavior for structural purposes, then the time dependence of this factor derives primarily from that of the relaxation modulus. It would stand to reason that in the event of such geometrical shapes the growth of the (imperfection) deformations would then be governed, at least to first order and before post-buckling deformations

† Because neither the bulk modulus nor the Poisson function is known for PMMA—nor, to our knowledge, for any polymer other than polyvinylacetate—there is really no other choice investigators have at this time than to make such an assumption; however, from the general behavior of these functions one has a good understanding of the consequences of making this assumption.

govern the response, by a function similar to that of the simple column problem. One might consider further, postulating a critical deflection as a failure criterion, that the failure time of the structure would be given by a curve "A" in Fig. 5, which is approximated in a rather conservative way by the relaxation function.

So far, we have treated only examples of time invariant loads. While there are many different kinds of load histories that may be considered, those of typical engineering interest are monotonically (linearly) rising loads and repeat on–off loading. The latter would correspond to typical load cycling experienced by an aircraft component under repeat use. Similarly, it would be of interest to consider cyclically varying temperatures in conjunction with similarly varying loads, simulating a typical loading cycle of the type encountered by future high speed aircraft.

We shall not develop the detailed responses for these kinds of loadings but point out that the solutions presented here provide first estimate bounds on the duration of such histories. In the event of repeat loads at constant temperature, the total deflection under repeat loading of, say, constant amplitude is smaller than the deflection resulting from constant load of the same magnitude. It follows that the total time required to achieve for the on–off load is given conservatively by the time for the constant load. In fact, it stands to reason that the growth of the deformations is governed primarily by the average axial load imparted to the column, rather than the maximal load if many cycles are involved; in initial examinations this is confirmed rigorously for simple material representations. We next turn to the comparison of the present model analysis with experimental results for constant end loads.

7. EXPERIMENTAL RESPONSE OF PMMA COLUMNS

Agreement between theoretical and experimental determination of buckling loads in "slender" elastic structures has met with varying degrees of success. For instance, the simply supported flat plate can withstand loads in excess of the (bifurcation) buckling load predicted by classical analysis (a result explained by von Karman) while the buckling loads of thin-walled cylinders at initial instability—but not necessarily for the whole post buckling response—may occur at loads less than one-third of classical predictions. The disagreements in these comparisons are normally due to two classes of inconsistencies between analysis and experiment: (1) geometric imperfections in the experimental structure (Koiter, 1945), and (2) inability to correctly model experimental boundary conditions (Babcock and Sechler, 1964; Hoff and Rehfield, 1965). The slowly loaded slender imperfect column, for which the buckling load is less than the yield load, begins to bend in response to moments induced by these geometric imperfections and load misalignment. However, the bending deformations remain small until the load approaches the Euler buckling load. If the column is subjected to axial displacement control, the load increases to a maximum and then remains virtually constant with increasing compressive displacement as fairly large deformations occur.

Since our problem is that of a slender column where the model is "exact" to within the restrictions of the kinematics of Euler buckling assumptions and the numerical solution of the equilibrium equations, experimental verification might seem unnecessary. However, to examine the agreement between our analysis and those of controlled, or perhaps uncontrolled, conditions in the laboratory, an experimental investigation is also reported here.

7.1. *Description of the experiment*

Specimens were held at constant, elevated temperature by electrical resistance heating elements in a commercially available temperature control cabinet. An MTS servo-hydraulic load frame was used to apply an initial load ramp and maintain a fixed end load for the remainder of the test. The lateral displacement at the column mid-span and the axial displacement of the actuator were measured using linear variable differential transformers (LVDT's) and all conditioned transducer outputs were recorded at uniform time intervals

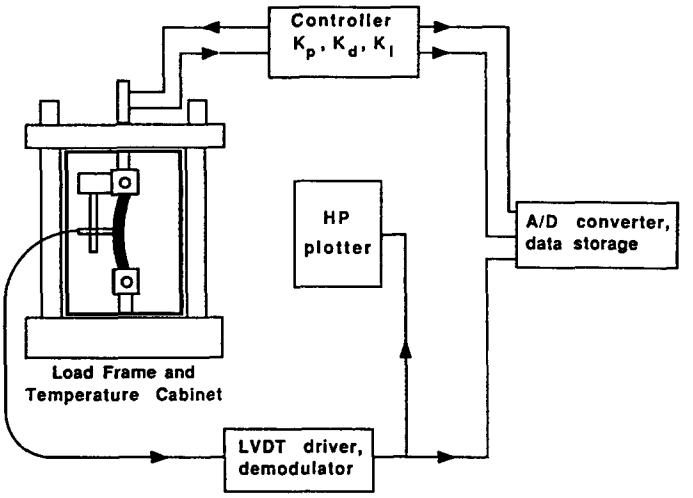

Fig. 9. Schematic of creep buckling experiment.

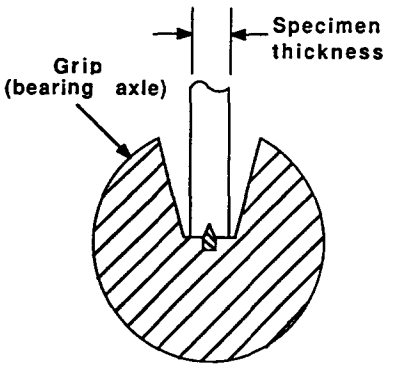

Fig. 10. Schematic of grip.

using a 12 bit A/D board on the hard disk of a micro-computer. A schematic of the experimental setup is shown in Fig. 9.

All specimens were machined from a cell cast sheet of commercially obtained PMMA (CYRO Industries Acrylite GP acrylic sheet).† The relaxation modulus was determined experimentally and is shown, at a reference temperature of 75°C together with a Prony–Dirichlet series approximation in Fig. 3. The specimens used were nominally 15.24 cm in length, 2.54 cm in width with a thickness of 0.635 cm. This geometry has a length to thickness ratio of 24 and a glassy buckling load of 658 Nt. Hinged end conditions were simulated at each end of the specimen by loading the specimen at the centerline of axles which are supported by a pair of ball bearings. Consistent load alignment was accomplished by notching each specimen end across the width at the mid-thickness which was then matched with a key that was press fit into the bearing axle keyway as shown in Fig. 10.

The experiments were conducted by first allowing the specimen and grips to reach thermal equilibrium at 75°C while the specimen was subjected to a small compressive preload ($\simeq 10$ Nt). The preload was necessary to maintain contact between the specimen and grips while thermal equilibrium was approached. A smooth load ramp was then initiated. The test duration was defined by limiting the lateral displacement at the specimen midspan to 2.0 cm. This displacement limit was set to prevent the specimen from snapping out of the grips when the bearing axle rotation became excessive.

† Reported to have an average molecular weight between 1.4 million and 2.0 million. No validation of the reported molecular weight was attempted.

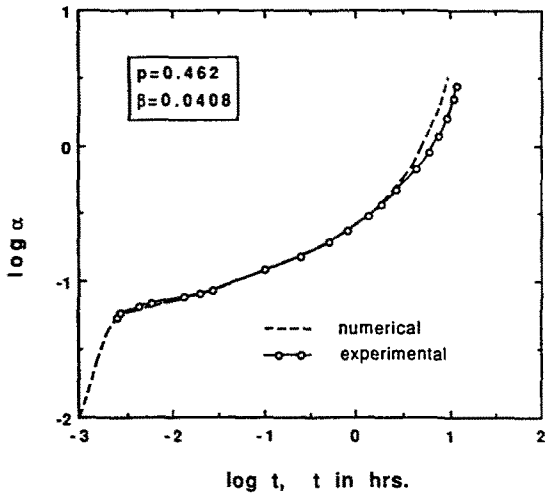

Fig. 11(a). Experimental results.

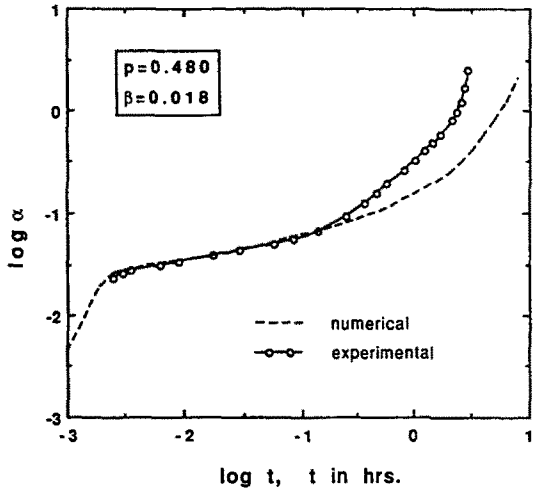

Fig. 11(b). Experimental results.

7.2. *Results and discussion*

A comparison of the numerical and experimental results is given for four different end loads in Fig. 11 (a)–(d). The numerical results were calculated using the geometrically linear model since this is adequate for the displacement levels allowed in the experiments (for further comments see below). In the figures the thickness-normalized lateral displacement at the midspan is plotted as a function of time including the portion derived from the initial ramp loading. Since the response $\alpha(t)$ is a linear function of the initial imperfection β the response to different initial imperfections can be determined by vertically shifting the response curves. Because it would have been difficult to measure the initial imperfections directly and independently,† this technique was used to determine them for the specimens tested. By including the initial load ramp in the numerical response the short term response of the numerical and experimental responses were matched, using the initial imperfection of the first mode as the fitting parameter. This procedure results in excellent agreement between theory and experiment during the slow growth phase. Even when the growth accelerates the model predicts the measured response reasonably well.

† Efforts to do so were made; however, the experimental involvement at a level of sufficient precision soon became disproportionate to the overall objective of the experimental work

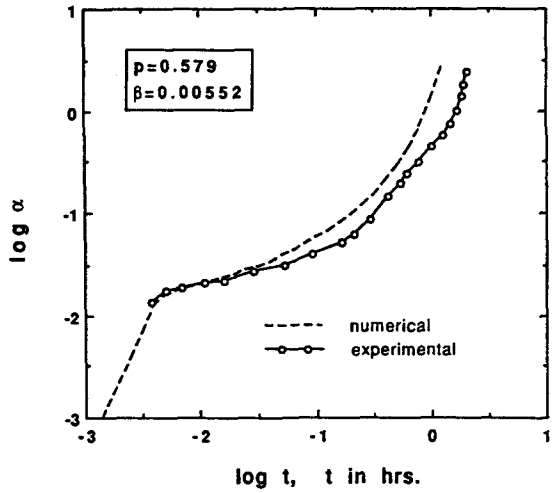

Fig. 11(c). Experimental results.

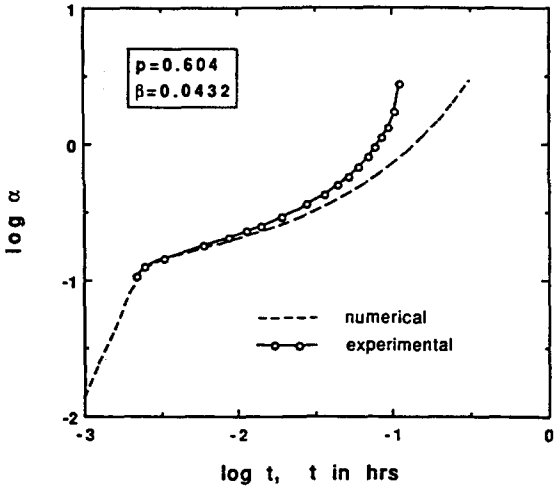

Fig. 11(d). Experimental results.

It can also be seen that when the theoretical and experimental results diverge at higher strain levels there is no consistency of error. That is, for the cases shown in Fig. 11 in the two cases (a) and (c), the model leads to larger deflections than were measured while in the other two, (b) and (d), the model results in smaller deflections than measured. These discrepancies cannot be explained through misalignment of load or non-linear material behavior. First, great care was taken to assure alignment consistency from test to test, and second, the method used to determine the initial imperfection, by its very nature, includes the effect of any load misalignment. It is also unlikely that the differences between theory and experiment derive from differences in boundary conditions since two mechanisms exist to inhibit the introduction of end moments to the column: the ball bearing grips and the cornered key used for load alignment.

The most likely explanation for the differences, in retrospect, is the variability in the material behavior associated with the uncontrolled residual stresses in the commercial PMMA which are not necessarily uniform over a large sheet as received. Material properties measurements on PMMA paralleling and following the present study have revealed that these residual stresses can be important and can account for distinct changes in the time dependent behavior. Even careful heat treatment (annealing) of the material has not been able to eliminate all the specimen-to-specimen variability in the time dependence. An additional factor possibly influencing the deviations seen in Fig. 11 is the temperature

variation experienced during testing. The environmental control unit was able to regulate temperatures to only $\pm 0.5°C$ and this could be improved only by using an additional chamber with a large thermal mass within the temperature control cabinet.

In this context, a comment is in order regarding the linear vs non-linear behavior of the test material. We first note that no crazing, a definite sign of tensile non-linear behavior, was apparent in any of the specimens. Next we observe that during the major portion of the deflection growth the strains were below 0.5%, rising only during the final stages to about 2% or above on the specimen surfaces. It is primarily during this last phase of the deformation histories that interaction between residual stresses in the material and the imposed deformations that non-linear effects could influence the time dependence of the deflection growth. No information on this type of behavior exists reliably for polymers in general, and for PMMA in particular. To further study this complicated material issue goes considerably beyond the immediate objective of the present study.

In summary, the linear model together with the use of a single parameter, which characterizes the geometric imperfection and load alignment, has been used to simulate creep buckling experiments in the laboratory. The short term and slow growth phases of the response are modeled reasonably well, while there exists some non-systematic variability in the representation of the final growth phase which is, most likely, due to yet generally poorly understood time dependent material behavior of polymers.

Acknowledgements—The authors would like to acknowledge the support of the National Aeronautics and Space Administration through grant number NSG1483 (Dr James Starnes technical officer). Also initial discussions on bifurcation formulations with Professor J. Singer (Technion) are gratefully acknowledged.

REFERENCES

Babcock, C. D. and Sechler, E. E. (1964). Effect of end slope on the buckling stress of cylindrical shells. NASA TN D-2537.

Biot, M. A. (1959). On the instability and folding deformation of a layered viscoelastic medium in compression. *J. Appl. Mech.* **26,** 393–400.

Biot, M. A. (1961). Theory of folding of stratified viscoelastic media and its implications in tectonics and orogenesis. *Geol. Soc. Am. Bull.* **72,** 1595–1620.

Bodner, S. R. (1991). A lower bound on bifurcation buckling of viscoplastic structures. *ASME Winter Annual Meeting*, Atlanta.

Flügge, W. (1975). *Viscoelasticity*. Springer, Berlin.

Freudenthal, A. M. (1946). Some time effects in structural analysis. *6th International Congress for Applied Mechanics*.

Halpin, J. C. and Meinecke, E. A. (1969). Delayed instability (buckling) of viscoelastic materials. U.S. Air Force Materials Laboratories Report, AFML-TR-68-331.

Hilton, H. H. (1952). Creep collapse of viscoelastic columns with initial curvatures. *J. Aero. Sci.* **19,** 844–846.

Hoff, N. J. (1954). Buckling and stability, 41st Wilbur Wright memorial lecture. *J. Roy. Aero. Soc.* **58,** 3–52.

Hoff, N. J. (1956). Creep buckling. *Aero. Quart.* **7,** 1–20.

Hoff, N. J. and Rehfield, L. W. (1965). Buckling of axially compressed circular cylindrical shells at stresses smaller than the classical value. *J. Appl. Mech.* **32,** 542–546.

Hopkins, I. L. and Hamming, R. W. (1957). On creep and relaxation. *J. Appl. Phys.* **28**(8), 906–909.

Huang, N. C. (1976). Creep buckling of imperfect columns. *J. Appl. Mech.* **E43**(1), 131–136.

Kempner, J. (1954). Creep bending and buckling of linear visco-elastic columns. NACA TN 3136.

Kempner, J. (1962). Viscoelastic buckling. In *Handbook of Engineering Mechanics* (Edited by W. Flügge), pp. 54-1–54-16. McGraw-Hill, New York.

Kempner, J. and Pohle, F. V. (1953). On the nonexistence of a finite critical time for linear viscoelastic columns. *J. Aero. Sci.* **20,** 572–573.

Koiter, W. T. (1945). Over de stabiliteit van het elastisck evenwicht (On the stability of elastic equilibrium). Thesis, Delft, H. J. Paris, Amsterdam.

Libove, C. (1952). Creep buckling of columns. *J. Aero. Sci.* **19**(7), 459–467.

Minahen, T. M. (1992). Structural instabilities involving time dependent materials: theory and experiment. Caltech thesis.

Schapery, R. A. (1962). Approximate methods of transform inversion for viscoelastic stress analysis. In *Proceedings 4th U.S. National Congress of Applied Mechanics*, pp. 1075–1085. New York.

Schapery, R. A. (1987). Viscoelastic buckling of an Euler-type beam. Texas A&M report, RR-87-03.

Sherwin, J. and Chapple, W. M. (1968). Wavelengths of single layer folds: a comparison between theory and observation. *Am. J. Sci.* **266,** 167–179.

Taylor, R. L., Pister, K. S. and Goudreau, G. L. (1970). Thermomechanical analysis of viscoelastic solids. *Int. J. Numer. Meth. Engng* **2,** 45–59.

Tvergaard, V. (1985). Rate sensitivity in elastic-plastic panel buckling. In *Aspects of the Analysis of Plate Structures* (Edited by D. J. Sawe and W. H. Horsington). Clarendon Press, Oxford.